Supplementary Information

Synthesis of a novel perovskite-carbon aerogel hybrid adsorbent with multiple metal-Lewis active sites for the removal of dyes from water; experimental and DFT studies

Daryoush Sanaei[1], Mohammad Hadi Dehghani[2,3], Hamidreza Sharifan[4], Monika Jain[5], Bahram Roshan[1], Javier A. Arcibar-Orozco[6*], Vassilis J. Inglezakis[7*]

[1]Department of Environmental Health Engineering, Faculty of Public Health and Safety, Shahid Beheshti University of Medical Sciences, Tehran, Iran

[2]Department of Environmental Health Engineering, School of Public Health, Tehran University of Medical Sciences, Tehran, Iran, Islamic Republic of

[3]Institute for Environmental research, Center for Solid Waste Research, Tehran University of Medical Sciences, Tehran, Iran, Islamic Republic of

[4]Department of Natural Science, Albany State University, Georgia, USA

[5] Department of Natural Resource Management, College of Forestry, Banda University of Agriculture and Technology, Banda- 210001

[6] Research Department, CIATEC A.C. Centro de Innovación Aplicada en Tecnologías Competitivas, León, Mexico

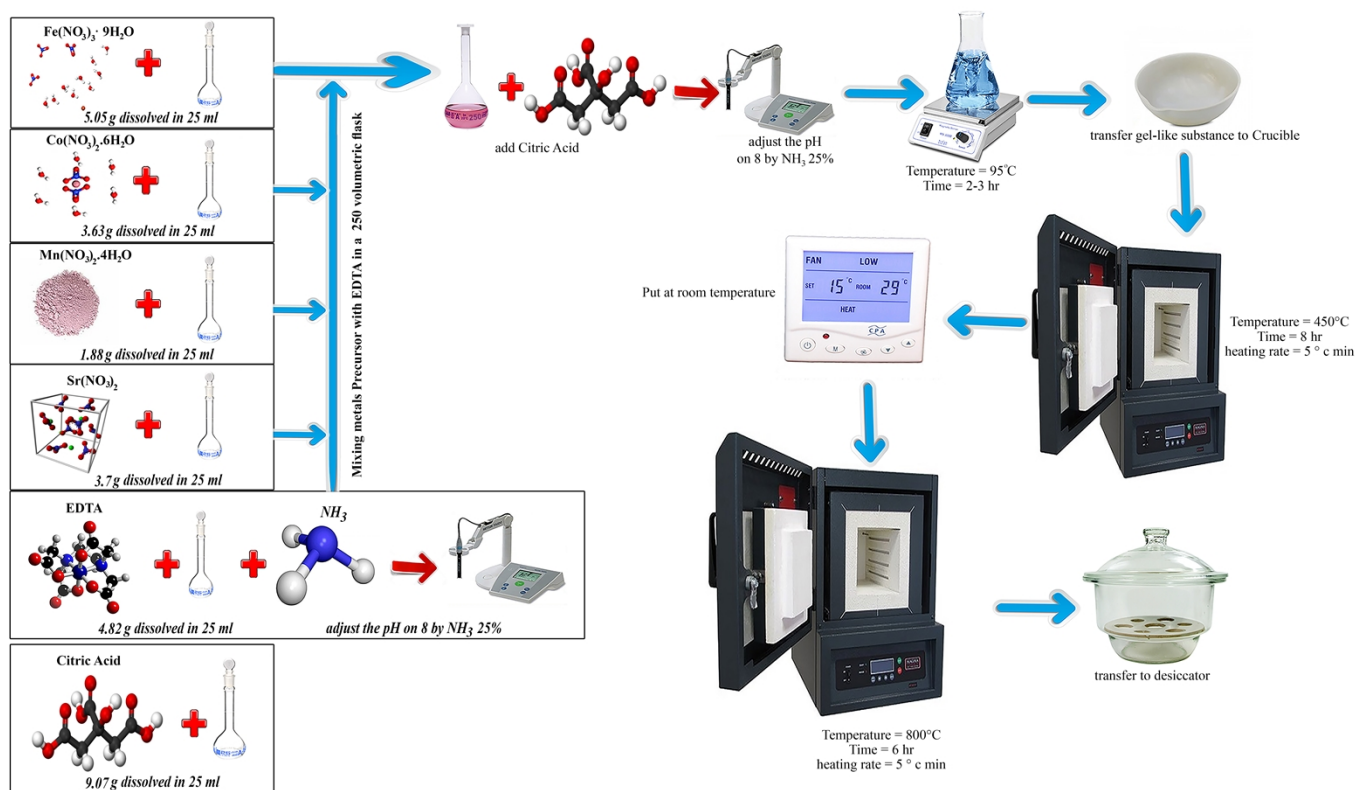[7]Department of Chemical & Process Engineering, University of Strathclyde, Glasgow, UK

vasileios.inglezakis@strath.ac.uk

Daryoushsanaei@gmail.com

hsharifan@tamu.edu

1. Experimental Section

Schematic explanation of the synthesis procedure of the DB-Perovskite/CAg Hybrid

Adsorbate preparation: In this work, the adsorbates were two cationic dyes, crystal violet (CV) and acid yellow 17(AY17), which were purchase from sigma Aldrich. For experimental study, a stock dye solution (1g L^{-1}) was provided by dissolving it's in Milli-Q water, which use for prepare the aqueous solution of these dyes. The UV-Vis spectrophotometer was used for determine dyes of concentration by measuring the absorbance of aqueous solution at maximum wavelength. For drawing the calibration curve for each dye using nine concentrations of dyes solutions of range from 0.1 mg L^{-1} to 15.0 mg L^{-1}. To ensure that calibration curve, this step was repeated three times. K_a values of dyes were calculated basic a standard method.

Desorption and regeneration studies: Desorption experiments were carried out to investigate the reversibility of CV and AY17 days from the DB-Perovskite/CAg Hybrid. The optimal values of adsorbent (0.05 g for CV and 0.1 g for AY17) were dissolved in 20 ml desorbing solvent 1 M HCl and HNO_3 for 24 h on a shaker. From UV-Vis spectrophotometer was used to measure the dyes desorbed. Regeneration studies were carried out to estimate the stability of DB-Perovskite/CAg Hybrid, for this purpose, the recovered adsorbent was dried at oven and then eluted with appropriate 1 M HCl and HNO_3 at 24 h and further regenerated in distilled water. Thereafter, the recycled DB-Perovskite/CAg Hybrid was used for the next adsorption experiments approximately, three adsorption cycles of adsorption-desorption process.

Density functional theory (DFT): The density functional theory (DFT) calculations carried out using The Vienna ab initio simulation package (VASP) with wave-based plane. Moreover, in order to explain the exchange-correlation, the general gradient approximation of Perdew-Burke-Ernzerhof (GGA-PBE) was used. A plane-wave basis of cut-off kinetic energy of 400 eV was performed to expand the smooth part of wave functions. A supercell with dimension of 5 *5*1 including 4 repeated units was used to simulate SA Fe-Mn/NH2-NHPCFB. For preventing periodic interaction, a 15 Å was used to set the vacuum layers. When the overall energy variation was smaller than 10^{-5} eV and all forces on each atom were less than 0.01 eV $Å^{-1}$, the relaxation of structures is stopped.

Thermodynamics study: To evaluate the impacts of temperature on CV and AY17 adsorption onto DB-Perovskite/CAg Hybrid and the nature of the adsorption process, the thermodynamic parameters, i.e., enthalpy ($\Delta H°$), the Gibbs free energy ($\Delta G°$), and entropy ($\Delta S°$), were investigated that calculated based to the following equations:

$$\Delta G^0 = - RTlnk \qquad \text{(S1)}$$

$$k = \frac{q_e}{C_e} \qquad \text{(S2)}$$

$$lnk = \frac{\Delta S^0}{R} - \frac{\Delta H^0}{RT}$$

(S3)

Where k_T is the equilibrium coefficient, C_e is the equilibrium concentration (mg L^{-1}), R is the universal gas constant (8.314 J mol^{-1} k^{-1}); and T is the solution temperature (K).

Adsorption isotherms: The Langmuir model used to estimate the adsorption performance, the formation of monolayer of dyes molecules on the adsorbent surface and the maximum adsorption capacity (Q_m) homogeneous surface of DB-Perovskite/CAg Hybrid due to adsorption process that written the linear and nonlinear forms it's as follows:

$1/q_e = 1/Q_m + 1/k_L Q_m . 1/C_e$ (S4)

$$q_e = \frac{Q_m K_L C_e}{1 + K_L C_e}$$

(S5)

To describe heterogeneous adsorption and the behavior of a multilayer adsorption on the DB-Perovskite/CAg Hybrid surface, Freundlich isotherm was researched that obtained from the equation follows:

Linear form

Ln q_e = Ln k_F + 1/n Ln C_e (S6)

Non-linear form

$$q_e = k_F C_e^{\frac{1}{n}}$$

(S7)

K_F is The Freundlich adsorption capacity and n is represented of adsorption heterogeneity.

To understand the nature of adsorption process, Dubinin–Radushkevich (D–R) isotherm was carried out. The equation of D–R isotherm is shown as:

Linear form

Ln (q_e) = Ln $(q_m) - \beta \varepsilon^2$ (S8)

Non-linear

$$q_e = q_m exp(-\beta\varepsilon^2)$$
(S9)

Where β is model constant connected to mean the free adsorption energy, q_m is the adsorption capacity (max) (mg g^{-1}), and ε is Polanyi potential of adsorption and is calculated as:

$$\varepsilon = RT \, Ln \, (1 + 1/C_e)$$
(S10)

T is the temperature of room condition (K), and R is the general gas constant (8.314 J/mol k). The mean free energy of adsorption (E) is given below:

$$E = 1/\sqrt{2\beta}$$
(S11)

We can use above equation to recognize the kind of adsorption process. In the values of E lower of 8 kJ mol^{-1}, the dominated process in adsorption is physisorption, E values of 8 to 16 kJ mol^{-1} is for ion-exchange and values of 20 to 40 kJ mol^{-1} is chemisorption process. Temkin model make the assumption that there is an interaction between adsorbate-adsorbent that can be shown as heat of adsorption. The Temkin equation is calculated as:

Linear form

$$q_e = B_T \, Ln \, K_T + B_T \, Ln \, C_e$$
(S12)

Non-linear

$$q_e = B_T \, (RT/b) \, Ln \, (K_T C_e)$$
(S13)

Where K_T is the maximum binding energy-based equilibrium constant and B_T is related to heat of adsorption.

Adsorption kinetics: The linear and Non-linear equations of pseudo- first order, pseudo-second-order, and Elovich were determined as follows:

Linear form

$$Ln \, (q_e - q_t) = Ln \, (q_e) - k_1.t$$
(S14)

$$\frac{t}{q_t} = \frac{1}{q_e^2 k_2} + \frac{1}{q_e}t$$
(S15)

$$q_t = \frac{1}{\beta}\ln(\alpha\beta) + \frac{1}{\beta}lnt$$

Non-linear form

$$\frac{dq_t}{dt} = k_1(q_e - q_t) \qquad\qquad (S16)$$

$$\frac{dq_t}{dt} = k_2(q_e - q_t)^2 \qquad\qquad (S17)$$

$$\frac{dq_t}{dt} = \alpha e^{-\beta_{qt}} \qquad\qquad (S18)$$

Where k_1, k_2, and α are the constant of pseudo-first, pseudo-second, and Elovich models, respectively. The β parameter is linked to the expanded coverage of surface and also activation energy for chemical adsorption (g mg^{-1}).

To realize the adsorption of mechanisms, other models such as Boyd, Bangham, and intraparticle diffusion are also investigated.

Boyd:

$$F = 1 - \left(\frac{6}{\pi^2}\right)exp(-Bt) \qquad\qquad (S19)$$

$$F = \frac{q_t}{q_e} \qquad\qquad (S20)$$

$$Bt = -0.4977 - ln(1 - F) \qquad\qquad (S21)$$

Where F is the adsorbed dyes into DB-Perovskite/CAg Hybrid at different times, Bt is function of F and other parameters are recently mentioned.

Bangham:

$$\log\left(\frac{C_0}{C_0 - q_t m}\right) = \log\left(\frac{k_0 m}{2.303V}\right) + \alpha log(t) \qquad\qquad (S22)$$

Where α (<1) and k_0 are Bangham constants, m is the used adsorbent (g L⁻¹), V is the volume of solution (mL) and other parameters are recently mentioned.

Intraparticle diffusion

$$q_t = k_{int}t^{1/2} + C \qquad\qquad (S23)$$

Where C and k_{int} are the intaparticle diffusion constant (mg g⁻¹ min⁻¹).

2. Supplementary Figures
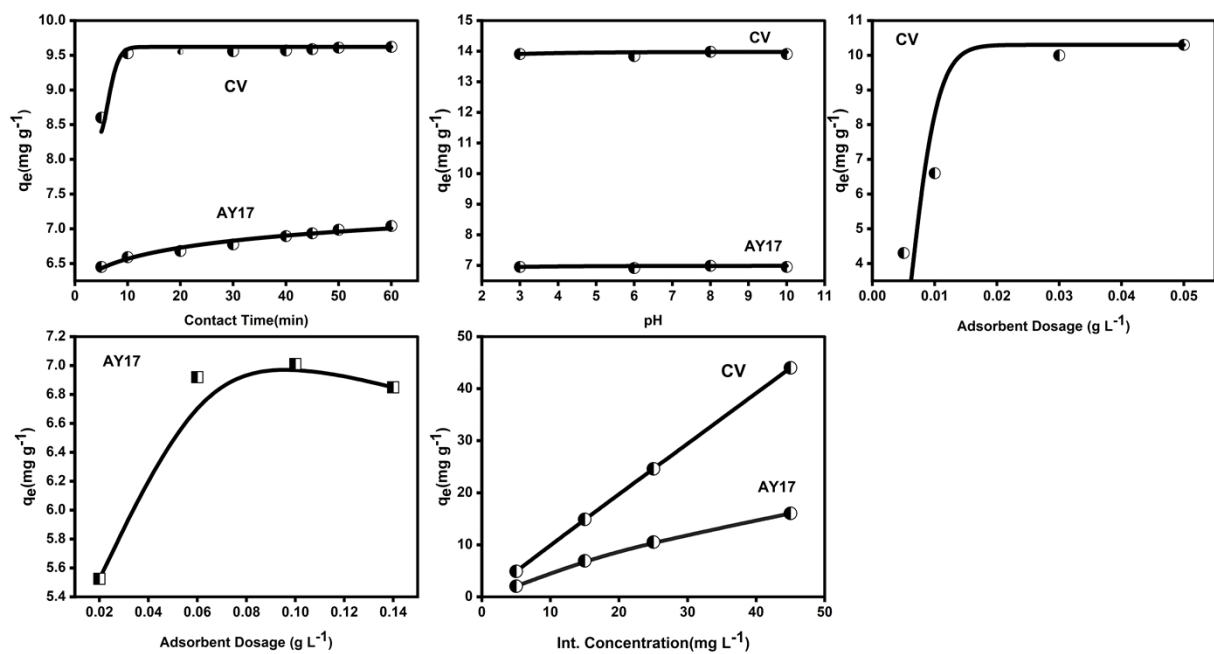
Supplementary Figure 1: the variable parameters influence on adsorption process in terms of a) time; b) initial concentration; c) adsorbent dosage; and d) pH.
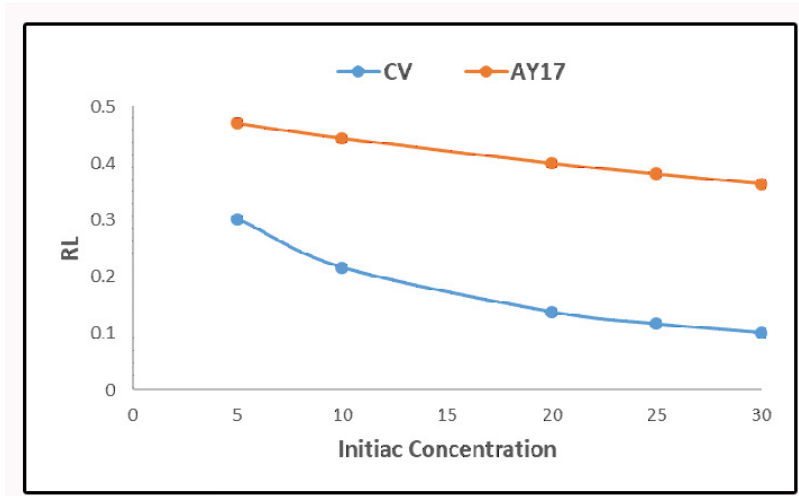
Supplementary Figure 2: Equilibrium parameter (Langmuir dimensionless) factor for DB-Perovskite/CAg Hybrid [pH (neutral); agitation speed (210 rpm); adsorbent dosage (0.1 g for AY17 and 0.05 g for CV; contact time (10 min for CV and 60 min for AY17); initial dyes concentration (5-40 mg L-1); volume of reaction (V = 50 mL); and temperature (25° C)].
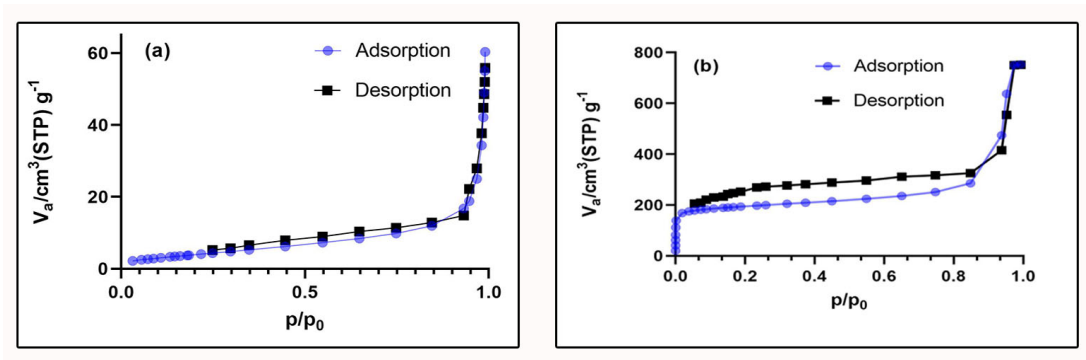
Supplementary Figure 3: Adsorption–desorption isotherms of nitrogen gas of (a) CAg and (b) DB-Perovskite/CAg Hybrid
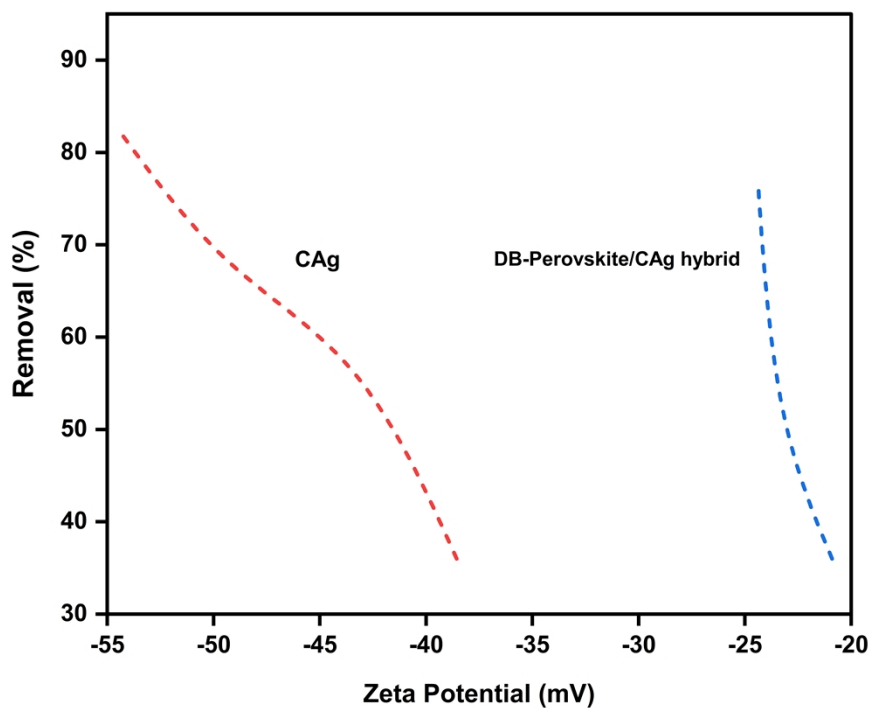
Supplementary Figure 4: *The performance of CV and AY17(co-adsorption) removal based on the corresponding Zeta Potential*
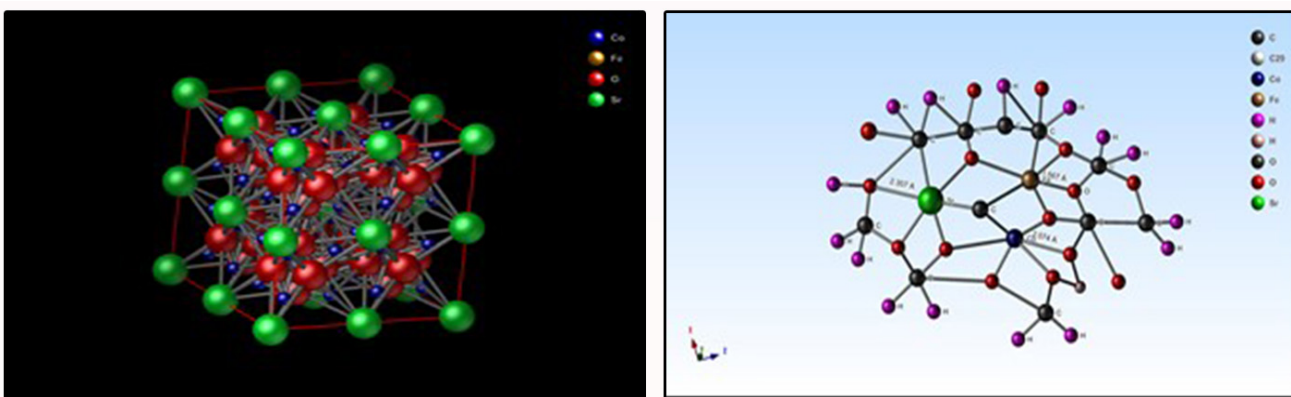
Supplementary Figure 5: The optimized geometry of the possible complexes.

3. Supplementary Table

Supplementary Table 1: The surface characteristics (relative concentration) of the catalysts calculated from the XPS spectra

Material	Surface concentration (proportion (Atomic %))					
	Sr 3d	Fe 2p	Co 2p	Mn 2p	O 1s	C 1s
double-B-sites perovskite /carbon aerogel hybrid	3.17	2.56	2.26	1.08	70.37	20.56

Supplementary Table 2: Isotherm model parameters and correlation (and error analysis) coefficients

Type of isotherms	CV	AY

Langmuir Parameters		
Q_{max} (mg g^{-1})	206	113.5
b (L mg^{-1})	0.79	0.23
R^2	0.99	0.97
X^2	253.16	893
ARE	15.83	46.9
$\Delta q\%$	70.97	12.5
Freundlich parameters		
k_f (mg g^{-1})/(mg L^{-1})^n	0.45	0.14
n	0.89	0.55
R^2	0.98	0.92
X^2	16592	2153
ARE	860.16	122.6
$\Delta q\%$	109.44	60.9
Dubinin–Radushkevich parameters		
Q_s (mg g^{-1})	12.73	4.46
k_{ad} (mol^2 kJ^{-2})	7.4	1.4
R^2	0.98	0.99
X^2	5310	320

ARE	261.28	4.19
Δq%	110.90	9.7
Temkin parameters		
B_T (J mole^{-1})	45.9	24.9
K_T (L g^{-1})	24.1	20
b (L g^{-1})	58.24	44.8
R^2	0.95	0.99
X^2	22524	774
ARE	1206	8.16
Δq%	111.33	10.6

Supplementary Table 3: Kinetic equation constants and correlation (and error analysis) coefficients at different concentrations

Pseudo- first order Parameters									
CV					AY				
Various concentration (mg L-1)	5	15	20	30	40	5	15	20	30	40
Q_e (exp)(mg g^{-1})	4.9	9.81	19.68	21.61	29.55	3.59	7.9	17.3	21.82	26.11
K_1 (min^{-1})	0.18	0.208	0.242	0.255	0.240	0.032	0.037	0.030	0.045	0.44
R^2			0.56					0.87		
X^2			328					16.66		
ARE			32.8					9.29		
Δq%			101.2					100.1		
Pseudo- second order parameters										
CV					AY					
Various concentration (mg L-1)	5	15	20	30	40	5	15	20	30	40

Q_e (exp)(mg g-1)	4.9	9.81	19.68	24.61	29.5	3.59	7.9	17.3	21.82	26.11
K_2 (g mg^{-1})/(min^{-1})	0.07	0.065	0.075	0.049	0.048	0.045	0.036	0.041	0.029	0.017
R^2			0.66					0.86		
X^2			314					25.1		
ARE			22.2					14.2		
$\Delta q\%$			90					104.2		
Elovich parameters										
			CV					**AY**		
Various concentration (mg L-1)	5	15	20	30	40	5	15	20	30	40
β (g mg^{-1})	1.01	099	0.78	0.65	0.42	0.76	0.79	0.59	0.11	0.08
R^2			0.946					0.941		
X^2			28.8					3.04		
ARE			2.76					0.26		
$\Delta q\%$			33					21.8		

Supplementary Table 4. Rate-determining mechanism constants and correlation (and error analysis) coefficients

	CV	AY
Intraparticle diffusion		
k_{int} *(mg g^{-1} min$^{-1/2}$)*	206	113.5
R^2	0.99	0.98
X^2	3893	50.2
ARE	206.87	8.94
Δq%	74.2	35.5
Bangham model		
R^2	0.98	0.99
X^2	276.2	174.5
ARE	14.45	10.44
Δq%	75.8	69.8
Boyd model		
R^2	0.94	0.96
X^2	6363	6137
ARE	315.1	365.6
Δq%	106.4	107.5

Supplementary Table 5. The BET surface area, pore volume and mean pore diameters of synthesized catalysts (DB-Perovskite/CAg hybrid) and carbon aerogel (CAg) obtained using N2 adsorption at 77 °K

Catalysts	BET surface area (m² g⁻¹)	Pore volume (cm³ g⁻¹)	Mean pore diameter (nm)
Carbon Aerogel	714.93	1.16	11.51
DB-Perovskite	22.681	0.312	24.86
DB-Perovskite/CAg Hybrid	390.23	0.75	16.51

Supplementary Table 6. The mass ratios of the DB-Perovskite/CAg hybrid adsorbent

Elt	Line	Error	W%	Absorption (A %)
Mn	Ka	0.7353	12.40	14.61
Fe	Ka	0.7353	27.17	31.48
Co	Ka	0.7353	25.76	28.30
Sr	La	1.0493	34.67	25.61
			100.00	100.00

Supplementary Table 7. The probable bonding of DB-Perovskite/CAg hybrid

Rank	Bond	d [Å]	d-Ratio
1	Fe O	0.82265	0.43298
2	Fe O	0.82265	0.43298
3	Fe O	0.82265	0.43298
4	Fe O	0.82265	0.43298
5	Fe O	0.82265	0.43298
6	Fe O	0.82265	0.43298
7	Fe O	0.82265	0.43298
8	Fe O	0.82265	0.43298
9	Fe O	0.82265	0.43298
10	Fe O	0.82265	0.43298
11	Fe O	0.82265	0.43298
12	Fe O	0.82265	0.43298
13	Fe O	0.82265	0.43298
14	Fe O	0.82265	0.43298
15	Fe O	0.82265	0.43298
16	Fe O	0.82265	0.43298
17	Fe O	0.82265	0.43298
18	Fe O	0.82265	0.43298
19	Fe O	0.82265	0.43298
20	Fe O	0.82265	0.43298
21	Fe O	0.82265	0.43298
22	Fe O	0.82265	0.43298
23	Fe O	0.82265	0.43298
24	Fe O	0.82265	0.43298
25	Fe O	2.28378	1.20199
26	Fe O	2.28378	1.20199
27	Fe O	2.28378	1.20199
28	Fe O	2.28378	1.20199
29	Fe O	2.28378	1.20199
30	Fe O	2.28378	1.20199
31	Fe O	2.28378	1.20199
32	Fe O	2.28378	1.20199
33	Fe O	2.28378	1.20199
34	Fe O	2.28378	1.20199
35	Fe O	2.28378	1.20199
36	Fe O	2.28378	1.20199
37	Fe O	2.28378	1.20199
38	Fe O	2.28378	1.20199
39	Fe O	2.28378	1.20199
40	Fe O	2.28378	1.20199
41	Fe O	2.28378	1.20199
42	Fe O	2.28378	1.20199
43	Fe O	2.28378	1.20199
44	Fe O	2.28378	1.20199
45	Fe O	2.28378	1.20199
46	Fe O	2.28378	1.20199

47	Fe O	2.28378	1.20199
48	Fe O	2.28378	1.20199
-	-	-	-
1	Co O	1.06967	0.61124
2	Co O	1.06967	0.61124
3	Co O	1.06967	0.61124
4	Co O	1.06967	0.61124
5	Co O	1.06967	0.61124
6	Co O	1.06967	0.61124
7	Co O	1.12856	0.64489
8	Co O	1.12856	0.64489
9	Co O	1.12856	0.64489
10	Co O	1.12856	0.64489
11	Co O	1.12856	0.64489
12	Co O	1.12856	0.64489
13	Co O	1.84761	1.05578
14	Co O	1.84761	1.05578
15	Co O	1.84761	1.05578
16	Co O	1.84761	1.05578
17	Co O	1.84761	1.05578
18	Co O	1.84761	1.05578
19	Co O	1.88231	1.07561
20	Co O	1.88231	1.07561
21	Co O	1.88231	1.07561
22	Co O	1.88231	1.07561
23	Co O	1.88231	1.07561
24	Co O	1.88231	1.07561
25	Co O	1.92230	1.09846
26	Co O	1.92230	1.09846
27	Co O	1.92230	1.09846
28	Co O	1.92230	1.09846
29	Co O	1.92230	1.09846
30	Co O	1.92230	1.09846
31	Co O	1.95568	1.11753
32	Co O	1.95568	1.11753
33	Co O	1.95568	1.11753
34	Co O	1.95568	1.11753
35	Co O	1.95568	1.11753
36	Co O	1.95568	1.11753
37	Co O	2.41563	1.38036
38	Co O	2.41563	1.38036
39	Co O	2.41563	1.38036
40	Co O	2.41563	1.38036
41	Co O	2.41563	1.38036
42	Co O	2.41563	1.38036
43	Co O	2.44228	1.39559
44	Co O	2.44228	1.39559
45	Co O	2.44228	1.39559
46	Co O	2.44228	1.39559

47	Co	O	2.44228	1.39559
48	Co	O	2.44228	1.39559
49	Co	O	2.46863	1.41065
50	Co	O	2.46863	1.41065
51	Co	O	2.46863	1.41065
52	Co	O	2.46863	1.41065
53	Co	O	2.46863	1.41065
54	Co	O	2.46863	1.41065
55	Co	O	2.49471	1.42555
56	Co	O	2.49471	1.42555
57	Co	O	2.49471	1.42555
58	Co	O	2.49471	1.42555
59	Co	O	2.49471	1.42555
60	Co	O	2.49471	1.42555
61	Co	O	2.84688	1.62679
62	Co	O	2.84688	1.62679
63	Co	O	2.84688	1.62679
64	Co	O	2.84688	1.62679
65	Co	O	2.84688	1.62679
66	Co	O	2.84688	1.62679
67	Co	O	2.86952	1.63973
68	Co	O	2.86952	1.63973
69	Co	O	2.86952	1.63973
70	Co	O	2.86952	1.63973
71	Co	O	2.86952	1.63973
72	Co	O	2.86952	1.63973
73	Co	O	2.89199	1.65481
74	Co	O	2.89199	1.65481
75	Co	O	2.89199	1.65481
76	Co	O	2.89199	1.65481
77	Co	O	2.89199	1.65481
78	Co	O	2.89199	1.65481
79	Co	O	2.89199	1.65481
80	Co	O	2.89199	1.65481
81	Co	O	2.89199	1.65481
82	Co	O	2.89199	1.65481
83	Co	O	2.89199	1.65481
84	Co	O	2.89199	1.65481
85	Co	O	2.91818	1.66531
86	Co	O	2.91818	1.66531
87	Co	O	2.91818	1.66531
88	Co	O	2.91818	1.66531
89	Co	O	2.91818	1.66531
90	Co	O	2.91818	1.66531
91	Co	O	2.91818	1.66531
92	Co	O	2.91818	1.66531
93	Co	O	2.91818	1.66531
94	Co	O	2.91818	1.66531
95	Co	O	2.91818	1.66531

96	Co O	2.91818	1.66531
97	Co O	2.94027	1.68016
98	Co O	2.94027	1.68016
99	Co O	2.94027	1.68016
100	Co O	2.94027	1.68016
101	Co O	2.94027	1.68016
102	Co O	2.94027	1.68016
103	Co O	2.96220	1.69269
104	Co O	2.96220	1.69269
105	Co O	2.96220	1.69269
106	Co O	2.96220	1.69269
107	Co O	2.96220	1.69269
-	-	-	-
1	Sr O	2.28627	0.90366
2	Sr O	2.28627	0.90366
3	Sr O	2.28627	0.90366
4	Sr O	2.28627	0.90366
5	Sr O	2.28627	0.90366
6	Sr O	2.28627	0.90366
7	Sr O	2.28627	0.90366
8	Sr O	2.28627	0.90366
9	Sr O	2.28627	0.90366
10	Sr O	2.28627	0.90366
11	Sr O	2.28627	0.90366
12	Sr O	2.28627	0.90366
13	Sr O	2.28627	0.90366
14	Sr O	2.28627	0.90366
15	Sr O	2.28627	0.90366
16	Sr O	2.28627	0.90366
17	Sr O	2.28627	0.90366
18	Sr O	2.28627	0.90366
19	Sr O	2.28627	0.90366
20	Sr O	2.28627	0.90366
21	Sr O	2.28627	0.90366
22	Sr O	2.28627	0.90366
23	Sr O	2.28627	0.90366
24	Sr O	2.28627	0.90366
25	Sr O	2.28627	0.90366
26	Sr O	2.28627	0.90366
27	Sr O	2.28627	0.90366
28	Sr O	2.28627	0.90366
29	Sr O	2.28627	0.90366
30	Sr O	2.28627	0.90366
31	Sr O	2.28627	0.90366
32	Sr O	2.28627	0.90366
33	Sr O	2.28627	0.90366
34	Sr O	2.28627	0.90366
35	Sr O	2.28627	0.90366
36	Sr O	2.28627	0.90366

37	Sr O	2.28627	0.90366
38	Sr O	2.28627	0.90366
39	Sr O	2.28627	0.90366
40	Sr O	2.28627	0.90366
41	Sr O	2.28627	0.90366
42	Sr O	2.28627	0.90366
43	Sr O	2.28627	0.90366
44	Sr O	2.28627	0.90366
45	Sr O	2.28627	0.90366
46	Sr O	2.28627	0.90366
47	Sr O	2.28627	0.90366
48	Sr O	2.28627	0.90366
49	Sr O	2.34220	0.92577
50	Sr O	2.34220	0.92577
51	Sr O	2.34220	0.92577
52	Sr O	2.34220	0.92577
53	Sr O	2.34220	0.92577
54	Sr O	2.34220	0.92577
55	Sr O	2.34220	0.92577
56	Sr O	2.34220	0.92577
57	Sr O	2.34220	0.92577
58	Sr O	2.34220	0.92577
59	Sr O	2.34220	0.92577
60	Sr O	2.34220	0.92577
61	Sr O	2.34220	0.92577
62	Sr O	2.34220	0.92577
63	Sr O	2.34220	0.92577
64	Sr O	2.34220	0.92577
65	Sr O	2.34220	0.92577
66	Sr O	2.34220	0.92577
67	Sr O	2.34220	0.92577
68	Sr O	2.34220	0.92577
69	Sr O	2.34220	0.92577
70	Sr O	2.34220	0.92577
71	Sr O	2.34220	0.92577
72	Sr O	2.34220	0.92577
73	Sr O	2.34220	0.92577
74	Sr O	2.34220	0.92577
75	Sr O	2.34220	0.92577
76	Sr O	2.34220	0.92577
77	Sr O	2.34220	0.92577
78	Sr O	2.34220	0.92577
79	Sr O	2.34220	0.92577
80	Sr O	2.34220	0.92577
81	Sr O	2.34220	0.92577
82	Sr O	2.34220	0.92577
83	Sr O	2.34220	0.92577
84	Sr O	2.34220	0.92577
85	Sr O	2.34220	0.92577

86	Sr O	2.34220	0.92577
87	Sr O	2.34220	0.92577
88	Sr O	2.34220	0.92577
89	Sr O	2.34220	0.92577
90	Co O	2.34220	0.92577
91	Co O	2.34220	0.92577
92	Co O	2.34220	0.92577
93	Co O	2.34220	0.92577
94	Co O	2.34220	0.92577
95	Co O	2.34220	0.92577
96	Co O	2.34220	0.92577

Supplementary Table 8. The characteristics of DB-Perovskite/CAg hybrid by Modified Pechini sol-gel obtained X-ray diffraction (XRD, STOE-STADV) that was accompanied by Cu-Kα Monochromatic Radiation ($\lambda = 1.54060$ Å) in a voltage of 40Kv and 40 mA electricity flow.

2Θ	hkl[1]	FWHM[2] (β)	Size of crystal[3] (nm)	d-spacing[4] (nm)
32.80	110	0.0036	40.76	0.272
44.33	111	0.0045	33.8	0.204
58.59	220	0.0036	44.2	0.157
64.47	300	0.0051	32.2	0.144
68.73	311	0.0036	44.8	0.136
	$V_{lattice}$ (Å^3)[5]	V_{atomic} (cm^3/mol) of Sr^{2+}	Lattice parameters	
DB-Perovskite/CAg Hybrid	174.11	33.72	a = 5.52	

[1]Miller index   [2]Full width at half maximum   [3]to calculate the size of adsorbent (crystalline size), Scherrer equation was used   [4]inter-atomic spacing   [5] cell lattice volume

References:

S1)   Hasan Z, Cho DW, Nam IH, Chon CM, Song H. Preparation of calcined zirconia-carbon composite from metal organic frameworks and its application to adsorption of crystal violet and salicylic acid. Materials. 2016 Apr; 9(4):261.

S2)   Chen X, Chin CJ. Adsorption and desorption of crystal violet and basic red 9 by multi-walled carbon nanotubes. Water Science and Technology. 2019 Apr 15; 79(8):1541-9.

S3)   Cheruiyot GK, Wanyonyi WC, Kiplimo JJ, Maina EN. Adsorption of toxic crystal violet dye using coffee husks: equilibrium, kinetics and thermodynamics study. Scientific African. 2019 Sep 1; 5:e00116.

S4)   Elella MH, Sabaa MW, ElHafeez EA, Mohamed RR. Crystal violet dye removal using crosslinked grafted xanthan gum. International journal of biological macromolecules. 2019 Sep 15; 137:1086-101.

S5)   Brião GV, Jahn SL, Foletto EL, Dotto GL. Adsorption of crystal violet dye onto a mesoporous ZSM-5 zeolite synthetized using chitin as template. Journal of colloid and interface science. 2017 Dec 15; 508:313-22.

S6)   Sabna V, Thampi SG, Chandrakaran S. Adsorption of crystal violet onto functionalised multi-walled carbon nanotubes: equilibrium and kinetic studies. Ecotoxicology and environmental safety. 2016 Dec 1; 134:390-7.

S7)   Doke KM, Yusufi M, Joseph RD, Khan EM. Comparative adsorption of crystal violet and congo red onto ZnCl2 activated carbon. Journal of Dispersion Science and Technology. 2016 Nov 1; 37(11):1671-81.

S8)   Miyah Y, Lahrichi A, Idrissi M, Boujraf S, Taouda H, Zerrouq F. Assessment of adsorption kinetics for removal potential of Crystal Violet dye from aqueous solutions using Moroccan pyrophyllite. Journal of the Association of Arab Universities for Basic and Applied Sciences. 2017 Jun 1; 23(1):20-8.

S9)   Garg D, Kumar S, Sharma K, Majumder CB. Application of waste peanut shells to form activated carbon and its utilization for the removal of Acid Yellow 36 from wastewater. Groundwater for Sustainable Development. 2019 Apr 1; 8:512-9.

S10)   Jedynak K, Wideł D, Rędzia N. Removal of rhodamine b (a basic dye) and acid yellow 17 (an acidic dye) from aqueous solutions by ordered mesoporous carbon and commercial activated carbon. Colloids and Interfaces. 2019 Mar; 3(1):30.

S11)   Njoku VO, Foo KY, Asif M, Hameed BH. Preparation of activated carbons from rambutan (Nephelium lappaceum) peel by microwave-induced KOH activation for acid yellow 17 dye adsorption. Chemical Engineering Journal. 2014 Aug 15; 250:198-204.